HIGH-TEMPERATURE DYNAMICS OF SURFACE MAGNETISM IN IRON THIN-FILMS

Pui-Wai Ma[1], C. H. Woo[1,*] and S. L. Dudarev[2,3]

[1]*Department of Electronic and Information Engineering, The Hong Kong Polytechnic University, Hong Kong SAR, China*

[2]*EURATOM/UKAEA Fusion Association, Culham Science Centre, Abingdon, Oxfordshire OX14 3DB, United Kingdom*

[3]*Department of Physics, Imperial College, Exhibition Road, London SW7 2AZ, United Kingdom*

ABSTRACT

Finite temperature magnetic properties of iron thin films are investigated, up to ferro/paramagnetic transition. The coupled dynamics of atoms and magnetic moments is treated using large-scale spin-lattice dynamics (SLD) simulations. A comprehensive study of surface and bulk magnetic properties is conducted, to investigate their dependences on temperature, film thickness, and crystallography of the film surface. We found that magnetization on the surface is enhanced at low temperatures, but is suppressed at higher temperatures, in agreement with experimental observations. The effective Curie temperature is found to decrease with the film thickness. Short-range magnetic order and non-vanishing spin-spin spatial correlations are observed above the Curie temperature. The spin autocorrelation functions exhibit slower oscillations with longer decoherence times near the surface. Directional spin disorder is found to have a significant effect on the surface strain.

*Corresponding email: chung.woo@polyu.edu.hk

1. INTRODUCTION

The surface of a crystal is a planar defect that strongly affects the properties of atoms located in its proximity. As a result, the presence of surfaces is expected to strongly influence the properties of systems with high surface to volume ratio, such as thin films and nano-particles. Accurate functional designs of magneto-electric devices often have to rely on the rigorous control of magnetic properties of ferromagnetic thin films at the operating temperature [1]. Thus, the link between magnetic and structural properties of magnetic metal films has attracted considerable attention [2]. Developing a good understanding of the effects of intrinsic and environmental variables, such as temperature, film thickness, surface crystallography, and applied stress, is not only technologically necessary, but also scientifically interesting. Despite experimental studies of surface magnetization [3]-[5] and structural relaxation [6]-[13] of ferromagnetic iron thin films at finite temperatures, little is known about the short range magnetic order (SRMO) near film or bulk metal surfaces. The dynamics of magnetism associated with temporal correlations and magnetic relaxation mechanisms, for example, still remains a difficult and poorly understood subject.

Theoretical models of surface magnetism have been based either on *ab-initio* [14]-[16] or magnetic many-body potential simulations [17], with a scope limited to relatively low temperatures, where the effects associated with *directional* spin wave degrees of freedom can be disregarded or treated as a small perturbation. A very limited amount of work has so far been devoted to the treatment of spin excitations at elevated temperatures, particularly in the ferromagnetic transition regime. Hasegawa [18] used a functional integral method and single-lattice-site approximation to treat the effect of spin fluctuations on the magnetism of the (100) surface in iron. However, the missing spin rotation-invariant term in the Hamiltonian [19] makes it difficult to address spin-wave excitations and SRMO effects. As a

result, the Curie temperature T_C was much overestimated, and the dynamics of magnetic moments left unaddressed. More recent models of magnetism of thin films [20],[21] are also subject to this limitation. *Ab-initio* calculations of surface relaxation [16],[22]-[24] omit dynamical effects of the phonon and magnon excitations. Conventional molecular dynamics (MD) simulations [17],[24] do not consider the *directional* spin degree of freedom, and do not treat the effect of spin wave excitation on the structure of the surface and vice versa. Both approaches are not equipped to treat ferromagnetism at elevated temperatures, particularly the interesting regimes near phase-transition.

The treatment of finite temperature magnetism has been advanced by the recent development of the spin-lattice dynamics (SLD) simulation scheme [25], within which one may consider, within a unified numerical algorithm, the combined effects of lattice relaxation, spin wave excitations, and lattice vibrations. All the degrees of freedom of atoms, including atomic coordinates, velocities, and directions of magnetic moments, are treated on equal footing as time-dependent variables. In this paper we investigate, by means of spin-lattice dynamics simulations, the atomistic dynamics of ferromagnetism in a thin film as a function of temperature, film thickness, and the crystallographic orientation of the surface. Magnetization of surface and bulk atomic layers is investigated as a function of temperature, and the effective Curie temperature of the film is calculated as a function of the thickness of the film.

Using spin-lattice dynamics simulations, we may also study the spatial and time spin-spin correlations that are directly related to the structure factor in neutron scattering [26]. The temperature-dependence of the surface SRMO of the film is studied in terms of the spin-spin spatial correlation function (SSCF) up to temperatures exceeding the Curie temperature for bulk iron $T_C \approx 1043K$. The oscillation and decoherence rates describing the evolution of the spin autocorrelation function (SACF) for the surface atoms is also examined.

At the same time the equilibrium magnetization is also studied as a function of proximity to the surface for various temperatures. We also examine the structural relaxation of the film, and show the significance of including the spin degrees of freedom in the treatment of relaxation at elevated temperatures.

2. SLD SIMULATION

The SLD simulation approach [25] treats atoms of iron as classical particles with intrinsic spins. Atoms interact via scalar many-body forces as in conventional MD, and they also interact via spin direction-dependent forces of the Heisenberg form. The corresponding classical Hamiltonian function for the system of interaction atoms is [25], [27]:

$$H = \sum_i \frac{\mathbf{p}_i^{\,2}}{2m_i} + U\left(\mathbf{R}\right) + \frac{1}{2}\sum_{i,j} J_{ij}\left(\mathbf{R}\right)\left(1 - \mathbf{e}_i \cdot \mathbf{e}_j\right) \qquad (1)$$

where the $\mathbf{e}_i$ is a unit vector of the direction of atomic spin. *U* is the potential energy of the atomic system $\mathbf{R} = \{\mathbf{R}_k\}$, for the case of perfect spin collinearity [24], i.e. for the case where $\mathbf{e}_i \cdot \mathbf{e}_j = 1$ for any pair of atoms *i* and *j*. The Dudarev-Derlet (DD) potential [28],[29] is used for *U*. An *ad-hoc* pair-wise inter-site exchange function J_{ij} describes the Heisenberg- type spin-direction-dependent contribution to the energy of the system, as defined in Ref. [25]. The lattice and spin degrees of freedom are coupled through J_{ij} and its derivatives. The equations of motion for atoms and spins are derived using the Poisson brackets [25]. We note that the current Hamiltonian does not include the demagnetization effect and the magnetic anisotropy energy. Therefore, the total energy of the spin subsystem is infinitely degenerate with respect to the choice of the system of coordinates describing the directional atomic spin degrees of freedom $\{\mathbf{e}_k\}$. Hence, while the specific direction of any atomic spin is immaterial, the *relative* orientation of neighboring spins, expressed in terms of spin

collinearity and spin-spin correlation functions, are significant and enter the Hamiltonian function (Eq. 1).

The notions of the spin thermostat and the spin temperature are introduced through the combined application of the Langevin spin dynamics [30],[31] and the fluctuation-dissipation theorem (FDT) [32],[33]. The FDT introduces temperature via a relationship between the random and dissipative forces. Such a relationship is obtained by solving the Fokker-Planck equation, and identifying the resulting energy distribution of the spin subsystem with the Gibbs distribution [25],[31]. The temperature dependence of the average magnetization for bulk bcc iron simulated using this method agrees well with experimental observations in the classical limit [25].

Since the magnetic moment vector of the i^{th} atom is given by $\mathbf{M}_i = -m_i \mathbf{e}_i$, the magnitude of the average of magnetic moment per atom, or the magnetization of the n^{th} atomic layer, can be written as $\left|\left\langle \mathbf{M}_i \right\rangle\right| = \frac{1}{N_n}\left|\sum_i \left(-m_i \mathbf{e}_i\right)\right| \approx \left\langle m_i \right\rangle \frac{1}{N_n}\left|\sum_i \mathbf{e}_i\right| \equiv \left\langle m_i \right\rangle \xi_C$, if we may neglect the statistical variation of m_i for atoms in the same layer. Here m_i is the magnitude of the atomic magnetic moment, which is found directly from the DD potential. Hence, to calculate the total magnetization at finite temperatures, one must take into account the loss of collinearity associated with the excitation of spin waves via the spin collinearity parameter $\xi_C = \frac{1}{N}\left|\sum_i \mathbf{e}_i\right|$ (see Ref. [25]). ξ_C is the statistical measure of directional order in the spin subsystem that characterizes the collective orientations of spins irrespective of the magnitude of the magnetic moments. Indeed, $\xi_C = 1$ describes the limit of fully collinear spin orientations, whereas $\xi_C = 0$ corresponds to a fully disordered spin configuration. A ferro/paramagnetic transition is an order/disorder transition that can be described in terms of ξ_C changing from a finite value to zero. This is different from the magnetic/non-magnetic transition in iron [34], which is associated with all the m_i vanishing as a result of change in

local electron density under applied external pressure.

In our SLD simulations we considered thin films of bcc iron with the (100), (110) and (111) surface orientations at temperatures of 100K, 300K, 700K, 1000K and 1200K. The starting configurations were prepared by extracting varying numbers of atomic planes from thermally equilibrated infinite bulk samples. The number of atoms in atomic planes parallel to the surface for the three cases were 900, 1296 and 504. Periodic boundary conditions were applied on the *x* and *y* directions. The dimension of each plane was approximately 85Å×85Å. The *x* and *y* dimensions of the simulation box, and the top and bottom surfaces were allowed to relax to a stress-free condition with total energy reaching equilibrium. The magnetic properties of the films were examined layer-by-layer in the direction normal to the surface of the film. To eliminate fluctuations, the data points were obtained by taking the average of data at 20 different time points, except for the case where time-correlation functions were investigated.

There is voluminous information available on iron thin films on copper substrates [2]. The film with (110) surface forms at room temperature if its thickness exceeds 11 monolayers. A thinner (110)-oriented film can also be formed by using a suitable copper-based alloy substrate, or by controlling the operating temperature [2]. Besides, experimental data on surface magnetization [3]-[5] are only available for the (110) surface, since this is the most energetically favorable surface orientation [24]. In what follows, if simulations show similar behavior for all the three types of surfaces, we describe results only for the (110) surface orientation. Wherever necessary, we also describe the results for the (100) and (111) surfaces.

3. SURFACE MAGNETIZATION

In Figure 1a we plot for each (110) atomic layer in a 36-layer film the averaged magnitude of atomic magnetic moments $\langle m_i \rangle$ (in unit of μ_B per atom) for various

temperatures. It can be seen that for all temperatures under consideration, $\langle m_i \rangle$ on the surface layer is always larger than that in the bulk. This behavior is independent of the film thickness, and is associated with the lower electron density due to the lower coordination number of atoms on the surface [28],[29]. Indeed, the $\langle m_i \rangle$ produced by both *ab-initio* [14]-[16] and magnetic potential [17] calculations also has the same behavior. It is also interesting to note that the value of $\langle m_i \rangle$ in the bulk of the film minimizes at 700K. This behavior is also found MD simulations of bulk iron using the DD potential. The general increase of $\langle m_i \rangle$ may be explained by the thermal expansion resulting in an effective on-site electron density reduction. The drop of $\langle m_i \rangle$ near 700K may be a special feature of the DD potential.

In Figure 1b, we show the spin collinearity parameter ξ_C for each atomic layer for various temperatures, surface orientations and film thicknesses. A common feature for all temperatures considered is the decrease of collinearity parameter ξ_C as we approach the surface from the bulk. This is due to the weakened action of the effective field on the spins, as the number of neighboring atoms is reduced by the presence of the surface. The mean magnetization $\left|\langle \mathbf{M}_i \rangle\right|$ for each atomic layer is shown in Figure 1c for various temperatures. $\left|\langle \mathbf{M}_i \rangle\right|$ can be seen to decrease rapidly as a function of temperature for T > 300K. It can also be seen that the magnetization is higher on the surface than in the bulk at temperatures below 300K, but the trend reverses at higher temperatures. This behavior can be understood when we consider the effects of two opposing temperature dependencies of $\langle m_i \rangle$ and ξ_C on $\left|\langle \mathbf{M}_i \rangle\right| \approx \langle m_i \rangle \xi_C$. Indeed, since the temperature dependence is independent of film thickness and surface orientation, the apparent disagreement between *ab-initio* results and the

experimental ones [3]-[5] is readily explainable on the temperature dependence of $\left|\langle \mathbf{M}_i \rangle\right|$, and that *ab-initio* results are valid only for very low temperatures, but not for the temperature at which the experiments are performed. Our results are consistent with those of Hasegawa [18] who suggested that the decrease of magnetization is due to the enhanced effect of spin fluctuations near the surface.

Figure 2 shows the atomic magnetic moment $\left|\langle \mathbf{M}_i \rangle\right|$ averaged over all the atoms in a film bounded by (110) surfaces, as a function of temperature for different film thicknesses. The magnitude of $\left|\langle \mathbf{M}_i \rangle\right|$ can be seen to vary strongly with the film thickness, especially in the high temperature regime. For example, at 1000K it increases five-fold from 0.11 μ_B per atom for a 4-layer film to 0.57 μ_B per atom for a 36-layer film. This effect weakens as temperature decreases, but it can still be detected even at 300K. From Figure 2, this results in a reduction of the Curie temperature T_C for thinner films. Razee *et al.* [21], who used the Korringa-Kohn-Rostoker (KKR) and coherent potential approximation (CPA) to evaluate the Curie temperature for the (100) film containing between 1 and 8 atomic layers also found similar behavior. Nevertheless, the Curie temperatures obtained in their calculations are much overestimated because of the reasons explained in the foregoing.

Figure 3 shows the layer-by-layer magnetization profiles for films of varying thicknesses for two temperatures: 1000K and 1200K. At 1000K, reduction of $\left|\langle \mathbf{M}_i \rangle\right|$ near the surface is seen for all film thicknesses. The presence of surfaces has a more significant effect on the total magnetization for the case of thin films, as expected. For very thin films the temperature dependence of $\left|\langle \mathbf{M}_i \rangle\right|$ no longer follows the temperature dependence of the bulk magnetization. When the temperature of the film exceeds the bulk Curie temperature, only a flat profile is observed (see the curves at 1200K). The remnant magnetization is

because ξ_C is positive definite [25].

4. THE SPIN-SPIN CORRELATION EFFECTS

Knowledge of the scattering structure factor is crucial in analyzing the dynamical properties of a material using neutron scattering. If treated as a function of the wave vector and frequency, the structure factor can be evaluated using the Fourier transform of the spatial and time correlation function. Studying these two correlation functions by means of direct simulations may assist with the treatment of surface effects and the interpretation of experimental observations, extending the possibility of experimentally probing the magnetic structure of thin films, and generally structurally complex materials, as opposed to the perfect crystal generally treated in theoretical analysis. From the SSCF and SACF, we can also deduce the SRMO and the decoherence time constant, respectively.

Figure 4 shows the SSCF, i.e. $\left\langle \mathbf{e}_i \cdot \mathbf{e}_j \right\rangle$, for the 1st and 2nd nearest neighbor (n.n.) atoms for each atomic layer of a thin film, for several films considered in this study. Although the average magnetization vanishes for temperatures higher than the bulk T_C, the local SRMO persists, similarly to the bulk crystal [25]. Our result shows that SSCF are weaker near the surfaces of a film. Yet, no matter how weak the effective field is, it appears to be sufficient to maintain the local SRMO, e.g., even at 1200K. The short range magnetic correlations are found to weaken with thinner samples. Indeed, the presence of a surface weakens magnetic correlations in a way somewhat similar to the effect of temperature.

Figure 5 shows the SACF, defined as $\left\langle \mathbf{e}_i(t) \cdot \mathbf{e}_i(t+\tau) \right\rangle = \sum_i \mathbf{e}_i(t) \cdot \mathbf{e}_i(t+\tau) / N$, for the 1st and the 2nd layers of a (110) films with 36 atomic layers for various temperatures. We start by examining the temperature effect on the SACF. For a (110) film, since only the surface layer shows a behavior significantly different to that of the bulk, we only plot the SACF for

the 1st and the 2nd layers. The oscillations in the SACF are due to spin rotations [25]. With increasing temperature, the equilibrium value (corresponding to the limit $\tau \to \infty$) of the SACF decreases, as expected. This is due to the increase in the transverse component of the spin orientation vector as a function of temperature. Comparison between the results for the 1st and the 2nd layer shows that the correlation function for the surface layer decreases faster, since the effective field acting on spins in this layer is weaker or, in other words, larger angle between the spin and the effective field is required to maintain the same energy distribution as in the bulk.

For other surface crystal structures, we plot, for 300K and 700K, the SACF of the first 5 atomic layers of the thickest films simulated in Figure 6. Although the general trends shown by the curves are similar, the differences in the number of nearest neighbors and the interlayer separation produce somewhat different behaviors. In general, the surface layers show the largest oscillations, lowest equilibrium value, and longest dephasing time. All these effects are caused by a weakened effective field on the film surface. In addition, since the (110) film has the most stable and compact surface, the behavior of this surface orientation is the closest to that of the bulk material. With the largest inter-layer spacing, the SACF does not show much change beyond the 2nd atomic layer. In comparison, all the first three layers are affected by the presence of the surface in (111) films.

Figure 7 shows the SACFs of the two surface layers on the (110) film at 300K and 700K, for various film thicknesses. It is clear that the SACFs are not much affected by the film thickness, showing that the SACFs are only function of their local atomic environments.

Finally, it is interesting to find out the role played by the spin degrees of freedom in the structural properties of a ferromagnetic surface. We do not attempt to be quantitative, since the DD potential was not parameterized using information about crystal surfaces. We study

the effects by using a film with 36 atomic layers bounded by the (110) surfaces. The interlayer relaxation strains $s_{12}(T) = \left(d_{12}(T) - d_{bulk}(T)\right)/d_{bulk}(T)$ for the 1st and 2nd atomic layers and $s_{23}(T)$ for the 2nd and 3rd atomic layers are plotted as a function of temperature in Figure 8. The relaxation strain s_{23} is tensile, and increases with increasing temperature. s_{12} is compressive at low temperature and becomes tensile at high temperatures. This is consistent with experimental measurements [7],[8] on a semi-infinite solid, from which s_{12} and s_{23} are both tensile, producing strains of 0.5~1% and 0.5%, respectively. Theoretical studies based on *ab-initio* calculations [15],[20],[22], on the other hand, report a 0.1~0.13% compressive strain for s_{12} and a 0.197~1.16 % tensile strain for s_{23} at 0K. Given the large experimental error band of ±2%, direct comparison with simulation results cannot be definitive. Yet, our finite temperature simulations do reveal trends not seen in the *ab-initio* calculations. In the insert in Figure 8, we compared our equilibrium interlayer spacing with those obtained using conventional MD simulation, in which the spin degrees of freedom were neglected. The visible difference between the curves highlights the significant effects of spin waves on lattice relaxation at high temperatures. Our analysis shows that for the case of a ferromagnetic material, it is essential to take full account of the spin-spin and spin-lattice correlated dynamics effects when developing effective interatomic potentials for simulating processes occurring at high temperatures.

5. CONCLUSIONS

The recently developed spin-lattice dynamics (SLD) simulation scheme is applied to large-scale dynamics simulations of magnetic properties of iron thin films. We investigate the magnetic properties of films as a function of temperature, film thickness, and surface crystallography. Effects of spin and lattice waves and their interactions are found to be particularly important at elevated temperatures. In all cases treated in this study, the overall

magnetization decreases with increasing temperature similar to the known bulk behavior, although the rate of this decrease varies as a function of film thickness. The temperature T_C for the order/disorder transition decreases as the film gets thinner. In all cases, surface magnetization is higher than bulk magnetization at low temperatures, but this behavior is reversed and surface magnetization becomes lower than that of the bulk at higher temperatures. The spin-spin spatial correlation function (SSCF) shows short range magnetic order that is less pronounced near surfaces, but persists at temperatures higher than the Curie temperature. The spin autocorrelation function (SACF) shows less rapid oscillations, longer decoherence times, and a lower asymptotic value for atomic layers close to the surface. The film with the (110) surface orientations shows behavior that most closely resembles that of crystal bulk. The thickness of film does not have a noticeable effect on this behavior. In comparison with conventional molecular dynamics simulations, where spin directional degrees of freedom are neglected, the near-surface relaxation strains exhibit qualitatively different behavior at elevated temperatures, hence showing the significance of including the treatment of spin-spin and spin-lattice correlations in the treatment of structural phase transitions occurring in magnetic materials at finite temperatures.

ACKNOWLEDGEMENT

This work is supported by Grants 532008 and 530507 from The Hong Kong Research Grant Commission. We also acknowledge support by the UK Engineering and Physical Sciences Research Council and by EURATOM. The views and opinions expressed herein do not necessarily reflect those of the European Commission.

Reference:

[1] U. Hartmann, *Magnetic Multilayers and Giant Magnetoresistance: Fundamentals and Industrial Applications*, Springer, Germany, 2000

[2] M. Wuttig and X. Liu, *Ultrathin Metal films: Magnetic and Structural Properties*, Springer, Germany, 2004

[3] L. N. Liebermann, D. R. Fredkin and H. B. Shore, Phys. Rev. Lett. 22 (1969) p.539

[4] J. C. Walker, R. Droste, G. Stern and J. Tyson, J. Appl. Phys. 55 (1984) p.2500

[5] J. Tyson, A. H. Owens and J. C. Walker, J. Appl. Phys. 52 (1981) p.2487

[6] K. O. Legg, F. Jona, D. W. Jepsen and P. M. Marcus, J. Phys. C: Solid State Phys. 10 (1977) p.937

[7] H. Li, Y. S. Li, J. Quinn, D. Tian, J. Sokolov, F. Jona and P. M. Marcus, Phys. Rev. B 42 (1990) p.9195

[8] C. Xu and D. J. O'Connor, Nucl. Inst. & Method in Phys. Research Sect. B 53 (1991) p.315

[9] H. D. Shih. F. Jona, U. Bardi and P. M. Marcus, J. Phys. C: Solid State Phys. 13 (1980) p.3801

[10] C. Xu and D. J. O'Connor, Nucl. Inst. & Method in Phys. Research Sect. B 51 (1990) p.278

[11] S. M. Yalisove and W. R. Graham, J. Vacuum Sci. & Tech. A 6 (1988) p.588

[12] J. Sokolov, F. Jona and P. M. Marcus, Phys. Rev. B 33 (1986) p.1397

[13] H. D. Shih, F. Jona, D. W. Jepsen and P. M. Marcus, Surf. Sci. 104 (1981) p.39

[14] O. Šipr and M. Košuth and H. Ebert, Phys. Rev. B 70 (2004) p.174423

[15] M. Chakraborty, A. Mookerjee and A. K. Bhattacharya, J. Magn. Magn. Mater. 295 (2005) p.210

[16] P. Błoński and A. Kiejna, Surf. Sci. 601 (2007) p.123

[17] P. Van Zwol, P. M. Derlet, H. Van Swygenhoven and S. L. Dudarev, Surf. Sci. 601 (2007) p.3512

[18] H. Hasegawa, J. Phys. F.: Met. Phys. 17 (1987) p.165

[19] H. Hasegawa, J. Phys. F.: Met. Phys. 13 (1983) p.1915

[20] R. Garibay-Alonso, J. Dorantes-Dávila and G. M. Pastor, Phys. Rev. B 73 (2006) p.224429

[21] S. S. A. Razee, J. B. Staunton, L. Szunyogh and B. L. Györffy, Phys. Rev. B 66 (2002) p.094415

[22] P. Błoński and A. Kiejna, Vacuum 74 (2004) p.179
[23] T. Kishi and S. Itoh, Surf. Sci 357 (1996) p.186
[24] M. J. S. Spencer, A. Hung, I. K. Snook and I. Yarovsky, Surf. Sci. 513 (2002) p.389; and reference therein
[25] P. W. Ma, C. H. Woo, S. L. Dudarev, Phys. Rev. B, 78 (2008) p.024434; P. W. Ma, C. H. Woo, S. L. Dudarev, in: A.S. Avilov *et al.* (Eds.), *Electron Microscopy and Multiscale Modelling, Proceedings of the EMMM-2007 International Conference*, (American Institute of Physics Conference Proceedings No. 999, AIP, 2008) p. 134.
[26] P. Schofield, Phys. Rev. Lett. 4 (1960) p.239
[27] S. L. Dudarev and P. M. Derlet, J. Comput.-Aided Mater. Des. 14, Suppl. 1 (2007) p.129
[28] S. L. Dudarev and P. M. Derlet, J. Phys.: Condens. Matter 17 (2005) p.7097; 19 (2007) p.239001.
[29] P. M. Derlet and S. L. Dudarev, Prog. Mater. Sci. 52 (2007) p.299
[30] W. F. Brown Jr., Phys. Rev. 130(1963) p.1677
[31] J. L. García-Palacios and F. J. Lázaro, Phys. Rev. B, 58 (1998) p.14937
[32] S. Chandrasekhar, Rev. Mod. Phys., 15 (1943) p.1
[33] R. Kubo, Rep. Prog. Phys., 29 (1966) p.255
[34] P. W. Ma, W. C. Liu, C. H. Woo and S. L. Dudarev, J. Appl. Phys. 101 (2007) p.073908

FIGURE CAPTIONS

Figure 1 (a) The average magnitude of atomic magnetic moments $\langle m_i \rangle$; (b) The collinearity parameter ξ_C; (c) magnetization $|\langle \mathbf{M}_i \rangle|$, evaluated for thin iron films bounded by the (110) surfaces. The films contain 36 atomic layers and the data show values for each atomic layer parallel to the surface of the film. Each point denotes the respective quantities averaged over the entire atomic layer. The atomic magnetic moments are given in μ_B per atom units.

Figure 2 The temperature dependence of magnetization of the whole thin film $|\langle \mathbf{M}_i \rangle|$ (in μ_B per atom units) for films containing 4, 7, 14 and 36 atomic layers.

Figure 3 Profiles of average magnetization $|\langle \mathbf{M}_i \rangle|$ (in μ_B per atom units) for films bounded by the (110) surfaces. Film thickness varied from 4, 7, 14 and 36 atomic layers, and simulations were performed for temperatures of 1000K and 1200K. Note the substantial reduction in the overall magnetization of the film as the thickness of the film decreases.

Figure 4 Through-thickness profiles of the spin-spin spatial correlation function (SSCF) average in the atomic planes parallel to the surfaces of the film for the (110) surface orientation for films containing 4, 7, 14 and 36 atomic layers at 1000K and 1200K. (Left) The SSCF for the 1st nearest neighbor. (Right) The SSCF for the 2nd nearest neighbor.

Figure 5 The spin autocorrelation function (SACF) evaluated for the 1st and the 2nd atomic layer for a film containing 36 layers of atoms. The surfaces of the film have the (110) orientation and curves are plotted for various temperatures.

Figure 6 The SACF for the first five atomic layers of films with the (110), (100) and (111) surfaces. Curves are plotted for temperatures of 300K and 700K.

Figure 7 The SACF for the 1st and 2nd atomic layers for the (110) films containing 4, 7, 14 and 36 atomic layers evaluated for 300K (left) and 700K (right).

Figure 8 The relaxation strain between the 1st and the 2nd atomic layers (s_{12}) and between the 2nd and the 3rd atomic layers (s_{23}) for the (110) film containing 36 atomic layers, shown as a function of temperature. The interlayer distances found in simulations are compared with

those evaluated using conventional MD (where no spin directional disorder effects are included). Note the significant effect of spin waves on surface relaxation.

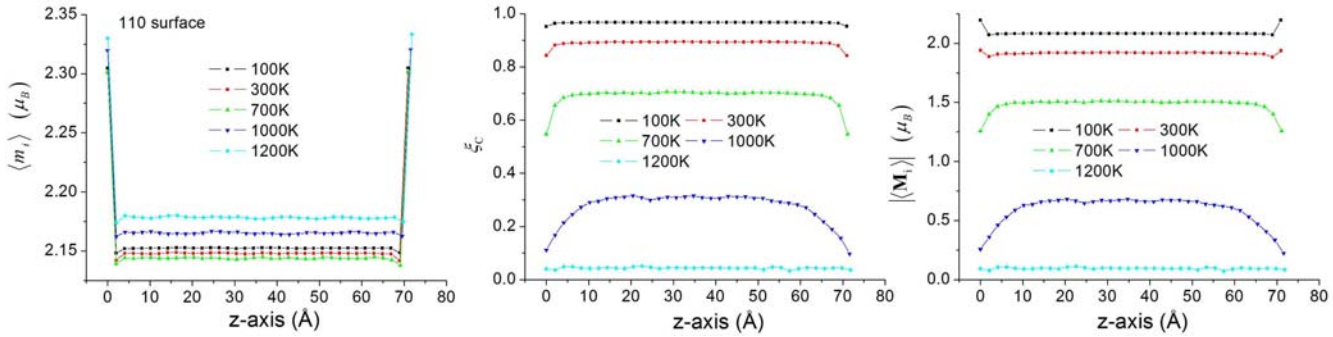

Figure 1

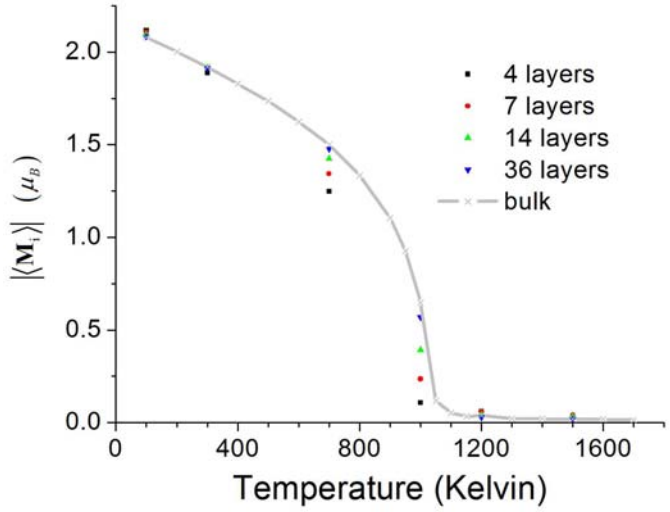

Figure 2

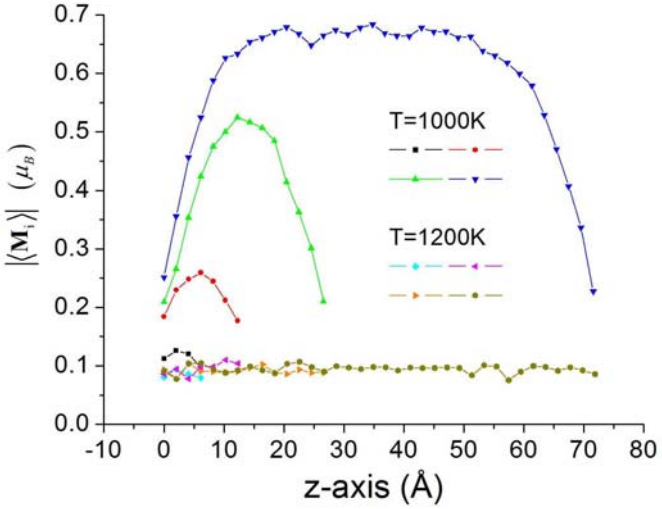

Figure 3

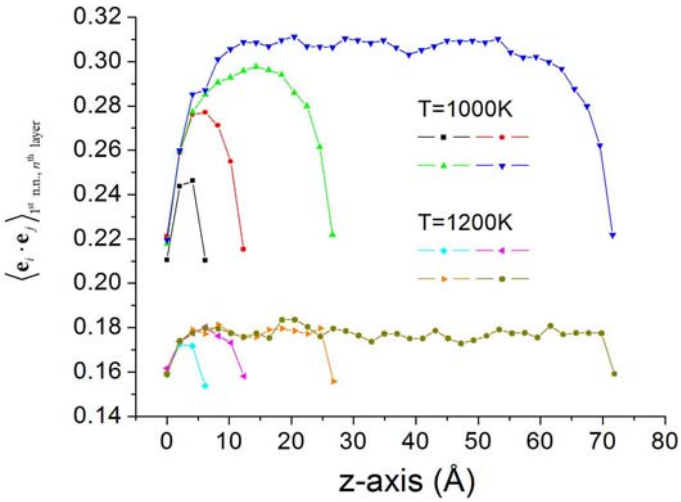

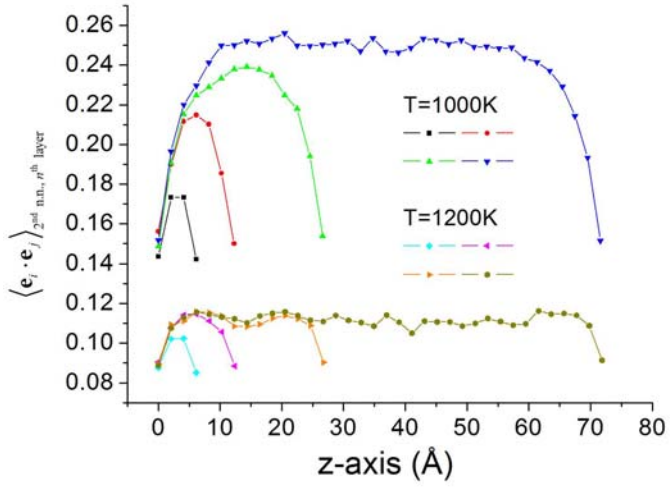

Figure 4

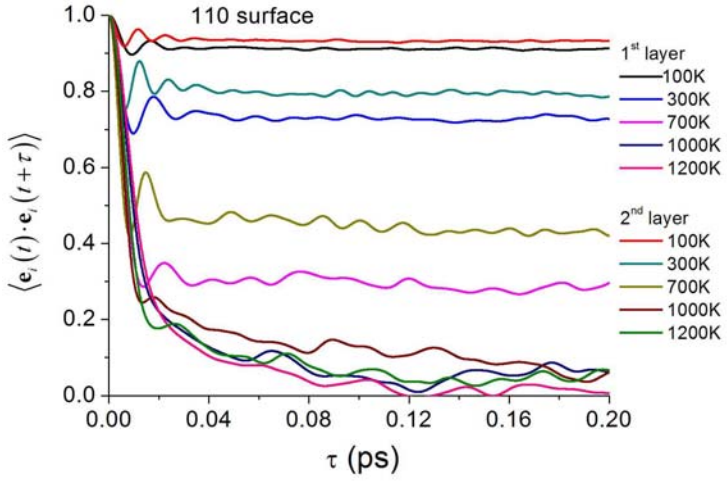

Figure 5

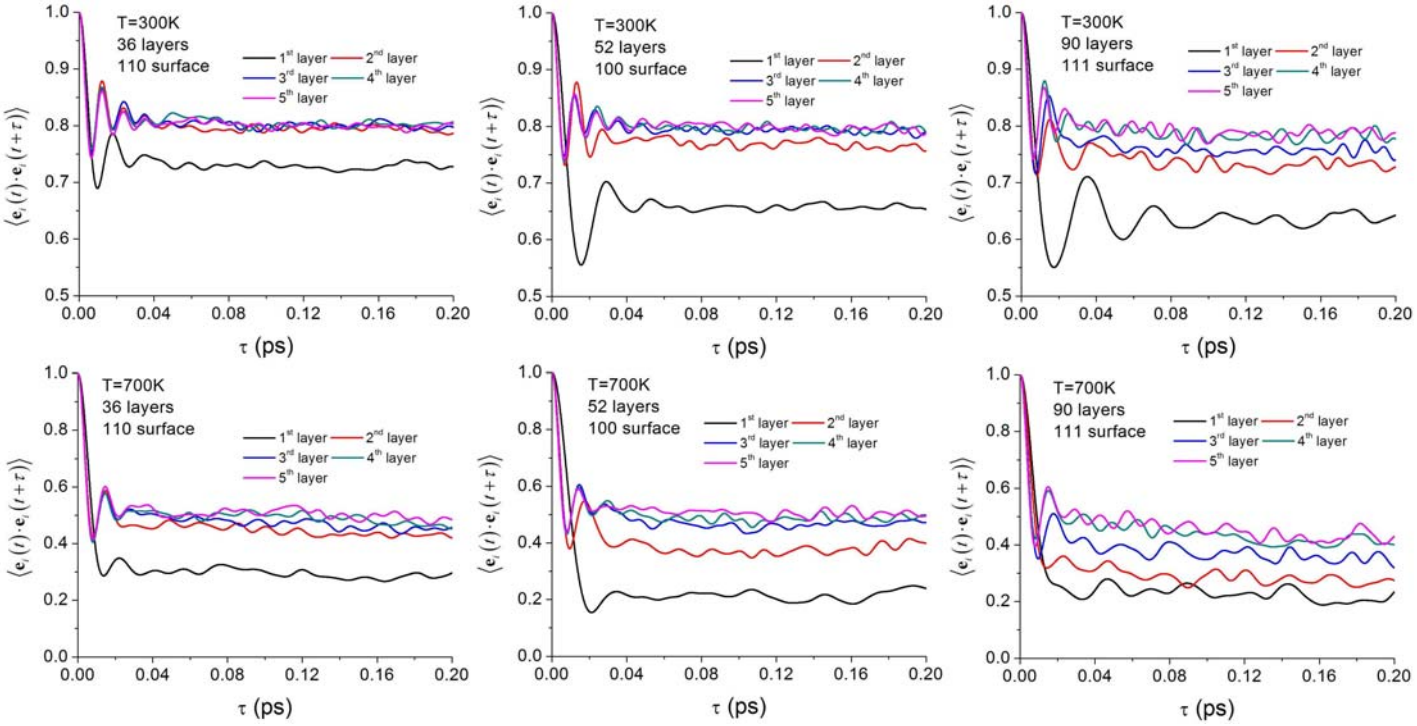

Figure 6

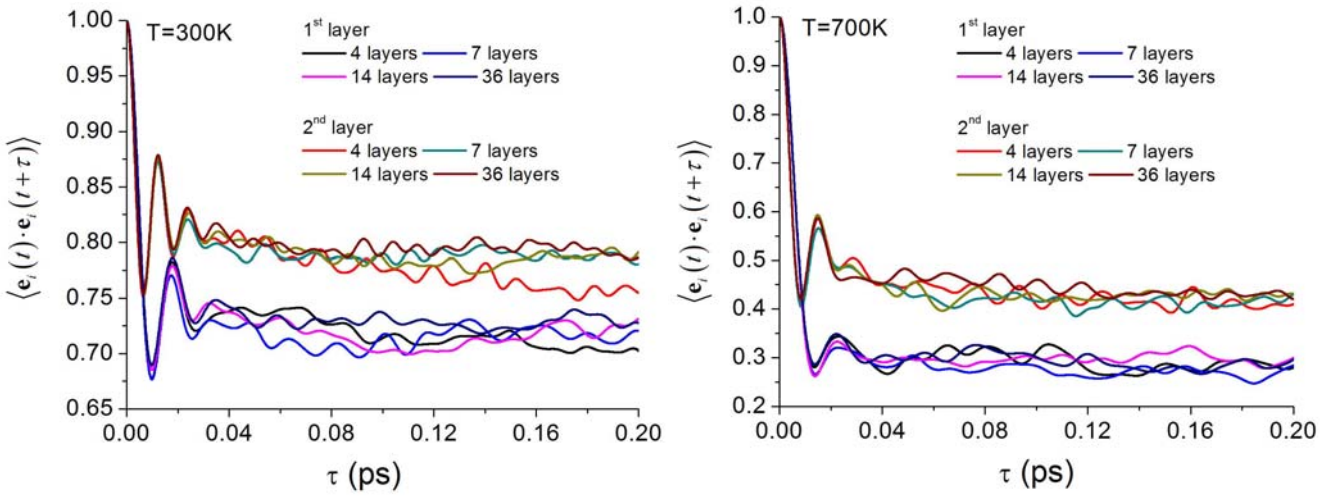

Figure 7

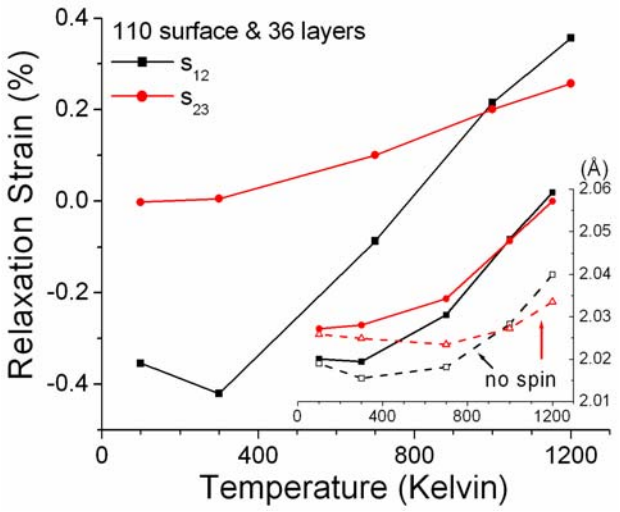

Figure 8